Accepted Manuscript

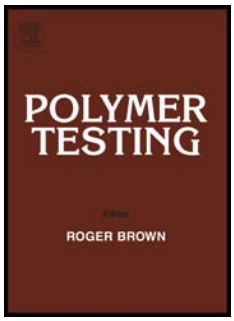

Broadband dielectric characterization of piezoelectric poly(vinylidene fluoride)thin films between 278 K and 308 K

L. Ciocci Brazzano, P.A. Sorichetti, G.D. Santiago, M.G. González

PII: S0142-9418(13)00136-0

DOI: 10.1016/j.polymertesting.2013.07.004

Reference: POTE 4084

To appear in: *Polymer Testing*

Received Date: 29 May 2013

Accepted Date: 12 July 2013

Please cite this article as: L.C. Brazzano, P.A. Sorichetti, G.D. Santiago, M.G. González, Broadband dielectric characterization of piezoelectric poly(vinylidene fluoride)thin films between 278 K and 308 K, *Polymer Testing* (2013), doi: 10.1016/j.polymertesting.2013.07.004.

Material Properties

Broadband dielectric characterization of piezoelectric poly(vinylidene fluoride)thin films between 278 K and 308 K

L. Ciocci Brazzano[1,2], P. A. Sorichetti[3], G. D. Santiago[1], M. G. González[1,2*]

1. Grupo de Láser, Óptica de Materiales y Aplicaciones Electromagnéticas (GLOMAE), Departamento de Física, Facultad de Ingeniería, Universidad de Buenos Aires, Paseo Colón 850, C1063ACV, Buenos Aires, Argentina.

2. Consejo Nacional de Investigaciones Científicas y Técnicas (CONICET)

3. Grupo de Sistemas Dispersos-Laboratorio de Sistemas Líquidos (GSD-LSL), Departamento de Física, Facultad de Ingeniería, Universidad de Buenos Aires, Paseo Colón 850, C1063ACV, Buenos Aires, Argentina.

Corresponding Author: M. G. González

* To whom correspondence should be addressed: (e-mail) mggonza@fi.uba.ar.

Abstract

This work describes the dielectric properties of piezoelectric poly(vinylidene fluoride) (PVDF) thin films in the frequency and temperature ranges relevant for usual applications. We measured the isothermal dielectric relaxation spectra of commercial piezoelectric PVDF thin films between 10 Hz to 10 MHz, at several temperatures from 278 K to 308 K. Measurements were made for samples in mechanically free and clamped conditions, in the direction of the poling field (perpendicular to the film). We found that the imaginary part of the dielectric relaxation spectra of free and clamped PVDF samples is dominated by a peak, above 100 kHz, that can be characterized by a Havriliak-Negami function. The characteristic time follows an Arrhenius dependence on temperature. Moreover, the spectra of the free PVDF samples show two additional peaks at low frequencies which are associated with mechanical relaxation processes. Our results are important for the characterization of piezoelectric PVDF, particularly after the stretching and poling processes in thin films, and for the design and characterization of a broad range of ultrasonic transducers.

Keywords

poly(vinylidene fluoride) – PVDF; piezoelectric thin films; ultrasonic transducers; medical imaging; broadband dielectric spectroscopy; clamped piezoelectric

1. Introduction

Poly(vinylidene fluoride) (PVDF) is a widely used semicrystalline polymer with good mechanical properties, resistance to chemicals, high dielectric permittivity and exceptional pyro- and piezoelectric properties [1,2]. Amongst other uses, thin films of piezoelectric PVDF are of great interest in broadband acoustic and ultrasonic transducers [3], particularly for medical imaging applications, since they are flexible and with acoustic impedance similar to water and biological tissues [4]. It is well known that quantitative modeling of the frequency response of piezoelectric transducers requires the accurate characterization of the material properties [5]. Compared to inorganic piezoelectric materials, the internal losses (both mechanical and electrical) are much larger in polymers. In consequence, it is very important to consider the frequency and temperature dependence of the relative complex dielectric permittivity, ε, when describing transducers based on piezoelectric polymers.

Numerous references may be found in the literature about the applications [6-9] and general physical properties of PVDF, particularly over limited ranges [9-15]. However, we found comparatively fewer works reporting in detail the broadband dielectric properties of piezoelectric PVDF thin films [16-18], especially in the frequency and temperature ranges required for the design and characterization of ultrasonic transducers. We note that most of those works do not take into account the difference between the behavior of piezoelectric materials in the free (zero-stress) and clamped (zero-strain) conditions.

In this work, broadband isothermal dielectric spectra of commercial piezoelectric PVDF thin films in the frequency range from 10 Hz to 10 MHz were obtained every 5 K between 284 K and 308 K. The electric properties were measured in the direction perpendicular to the film. These ranges cover most of the usual medical imaging applications [19]. Measurements were made both in the free and clamped conditions. As is clear from rheological considerations, the free dielectric response of piezoelectric materials is significantly changed when the sample is clamped, since the interaction between the electrical and mechanical responses is eliminated [20,21]. This is an aspect [22] that is often overlooked in studies of properties of electrorheological materials. Moreover, the dielectric spectra presented in this work are important for the characterization of piezoelectric PVDF, particularly, after the stretching and poling processes in thin films.

2. Materials and methods

Circular samples about 6mm in diameter were cut from piezoelectric PVDF film 25 μm thick, metalized on both sides, provided by PIEZOTECH CORP. During manufacture, the film is stretched and then poled by applying an electric field in the direction perpendicular to the film. The poling direction is customarily indicated as the reference axis 3 and the stretching direction (in the plane of the film) as the reference axis 1. In this work, we measured the dielectric properties in the direction of the poling field, ε_{33}. For brevity, the subscript '33' will be omitted in what follows.

Electrical connections to the free sample were made with two short (5 mm) copper wires of small diameter (100 μm), bonded to the periphery of the metalized surfaces of the sample with speckles of conductive silver paint. The clamped sample was placed between two thick metallic disk electrodes tightly held together.

The samples were placed in a glass enclosure flushed with dry nitrogen, in a Lauda thermostatic bath

stabilized within +/- 0.02 K. The temperature was measured to within +/- 0.1 K with a calibrated thermocouple placed next to the sample. The temperature at the laboratory was stabilized at 299 K +/-1 K.

The samples in the thermostat were connected to the dielectric measuring interface with a short length (1 m) of low-loss coaxial cable (with a nominal impedance of 50 Ω). The impedance and propagation delay of the cable were accurately determined with an automated reflection bridge at frequencies up to 30 MHz. We emphasize that the accurate characterization of the cable is essential to correct the systematic errors in measurements at high frequencies, where the cable length is not negligible in comparison to the signal wavelength.

The dielectric measuring interface, together with the measurement method and the calibration procedures, were described in detail in a previous work [23].

At low frequencies, between 10 Hz and 100 kHz, a Stanford Research SR-810 Lock-in Amplifier was used for magnitude and phase measurements, using its internal source to provide the excitation signal. In the frequency range from 20 kHz to 10 MHz, signals were captured with a Tektronix TDS 210 real-time digital sampling oscilloscope, and processed with an FFT routine. The excitation signal was provided by an Instek GW-830 synthesized signal generator. We checked the overlap of experimental results from both sets of instruments in the frequency range between 20 kHz and 100 khz. As an additional verification, we made measurements at 1 kHz, 10 kHz and 100 kHz using a stand-alone Tonghui 2822C RCL Meter.

Results at frequencies above 100 kHz were corrected with the usual formulas for low-loss transmission lines [24], using the impedance and propagation delay data of the coaxial cable. The instruments were controlled by a personal computer through GPIB interfaces, and the software for instrument control and signal processing was developed using the Agilent VEE environment. In all cases ceramic reference capacitors were used for calibration.

3. Results and Discussion

The complex relative permittivity characterizes the macroscopic response of the material to electric fields with a harmonic time dependence. As described in the previous section, we measured the dielectric properties for the free and clamped samples. Figures 1 to 4 show the real and imaginary parts of the relative complex permittivity (as a function of frequency) for both samples. Results are shown only for three of the measured temperatures. The imaginary part of the dielectric relaxation spectra of both the free and clamped PVDF samples is dominated by a peak above 100 kHz.

As it can be seen from the low-frequency behavior, the zero-frequency (DC) conductivity of the samples may be neglected. We emphasize that, if that were not the case, the imaginary part of the permittivity at low frequencies would exhibit a characteristic ω^{-1} dependence that is clearly absent from our experimental data (see, for instance, figure 4).

The Cole-Cole plots (imaginary vs. real part of the complex permittivity) for the same temperatures are given in Figures 5 and 6. We note that the spectra of the free PVDF samples show two additional relaxation processes at low frequencies, that are absent from the spectra of clamped samples. This is not surprising since in piezoelectric materials the mechanical and electrical responses are coupled and, therefore, the mechanical relaxation processes clearly dominate the measured low-frequency dielectric losses in free PVDF (below 100 kHz). Low frequency losses in the free condition cannot be neglected and increase with temperature. In contrast, in the clamped condition, low-frequency losses are very low in the entire range of measured temperatures.

The piezoelectric constitutive equations for isothermal processes are [25]:

$$\begin{aligned} x &= s^{T,E} \cdot X + d^{T,X} \cdot E \\ D &= d^{T,E} \cdot X + \varepsilon_0 \cdot \varepsilon^{T,X} \cdot E \end{aligned} \tag{1}$$

where the independent variables are *x* the strain field, *X* the stress field, *E* the electric field, and *D* the displacement field. Furthermore, *s* is the elastic compliance tensor, *d* the piezoelectric tensor and ε the dielectric tensor. The superscripts indicate which variable keeps constant (temperature, *T*, electric or stress field). ε_0 is the free space permittivity. A harmonic time dependence is assumed, therefore all the above parameters depend on the frequency and may be considered as complex [26]. Please note that in this work we only measured the components along the reference axis 3.

As explained in reference [25], from the comparison with the results of the sample in a clamped condition (i.e. the strain, *x*, is negligible) it can be deduced that the measured complex permitivitty for a free sample includes the electromechanical coupling with the strain through the piezoelectric coefficients *d*:

$$\varepsilon^{T,X} = \varepsilon^{T,x} + \left(d^{T,E} \cdot d^{T,X}\right) / \left(\varepsilon_0 \cdot s^{T,E}\right) \tag{2}$$

It is useful to consider the elastic modulus, *G*, defined as the reciprocal of the elastic compliance. Therefore, for the previous equation it follows that:

$$\varepsilon^{T,X} - \varepsilon^{T,x} = d^{T,E} \cdot d^{T,X} \cdot G^{T,E} / \varepsilon_0 \tag{3}$$

From the above, it may be seen that the difference between the free and clamped permittivities depends on the mechanical properties of the sample through G; this is highlighted in the plots of figures 7 and 8. The imaginary part shows a peak between 1 kHz and 10 kHz and the side of another peak below 100 Hz that shifts to higher frequencies with increasing temperature.

The high frequency peak in the dielectric loss is originated by the β relaxation process, attributable to fluctuations of the dipolar moment of localized parts of the main polymer chain [27]. This peak can be described by a Havriliak-Negami (HN) function [28],

$$\varepsilon = \varepsilon_{HF} + \Delta\varepsilon / \left[1 + \left(j \cdot \omega \cdot \tau_0\right)^{\gamma}\right]^{\delta} \tag{4}$$

where ε_{HF} is the limiting value of the permittivity at high frequencies, $\Delta\varepsilon$ the relaxation strength, τ_0 the characteristic relaxation time, and γ and δ are shape parameters that describe the broadening of the relaxation peak. The shape parameters are related to symmetric and asymmetric broadening of the relaxation peak, and they are both positive numbers (for a relaxation processes the product $\gamma \cdot \delta$ must always be less than 1 [27]. The HN function is a generalization of the single-time (Debye) relaxation

function. The dynamical response of a Debye process is described by $\gamma = \delta = 1$; this corresponds to an exponential decay of the polarization. In contrast, $\gamma < 1$ implies a relaxation peak symmetrically broader than a Debye peak, and $\delta < 1$ implies a nonsymmetric broadening of the relaxation peak. In the time domain this corresponds to a decay of the polarization described by a "stretched exponential" function [27].

The HN parameters for the main relaxation peak at each measured temperature are given in tables 1 and 2 for the free and clamped samples, respectively. In figures 1 to 6, the solid lines correspond to the HN function with the fitting parameters from tables 1 and 2. In all cases, the root-mean-square error (RMSE) in the fitting is less than 0.3. The activation energy is of (0.81+/-0.21) eV for the free sample, and (0.74+/-0.11) eV for the clamped sample. The uncertainties correspond to 95 % confidence interval. We present the Arrhenius plots of the characteristics times in figures 9 and 10. It is well known that the Arrhenius dependence of the relaxation time is a typical feature of the β relaxation, together with the increase of the relaxation strength with temperature [27]. It is important to note that the dielectric relaxation peak corresponding to the α process is well below the minimum measured frequency, within the temperature range studied in this work.

4. Summary

We performed broadband isothermal spectroscopy in samples of PVDF thin films in the frequency range from 10 Hz to 10 MHz, and for temperatures between 284 K and 308 K. The samples were measured along the direction of the poling field, in the free and clamped conditions. The β relaxation process dominates the electric losses above 100 kHz. The temperature dependence of the relaxation times are well described by an Arrhenius process and the fitted activation energies for the free and clamped condition are similar (0.81 eV and 0.74 eV, respectively). We have not found in the literature parameters of the β relaxation process obtained from broadband isothermal dielectric spectra. The zero-frequency DC conductivity of the samples may be considered as negligible. The spectra of the free PVDF samples show two additional relaxation processes at low frequencies, originated by the electromechanical coupling with the mechanical relaxation. In contrast, low frequency losses in the clamped condition are very low.

Widespread application of piezoelectric polymers requires a detailed description of dielectric properties in the range of frequencies and temperatures of interest, both in the free and clamped conditions. The results presented in this work are relevant for the characterization of piezoelectric PVDF thin films and for the design and characterization of a broad range of ultrasonic transducers, such as hydrophones and medical imaging systems.

Acknowledgements

This work was supported by the University of Buenos Aires, grants UBACYT-20020100300035, UBACYT-20020090100136 and UBACYT-20020100100406; Consejo Nacional de Investigaciones Científicas y Técnicas (CONICET), grant PIP-112-201101-00676; and the Agencia Nacional de Promoción Científica y Tecnológica, grant PICT-2011-01211. Also, a post-doctoral grant from CONICET for one of the authors is gratefully acknowledged.

References

[1] M.G. Broadhurst, G.T. Davis, J.E. McKinney, R.E. Collins. Piezoelectricity and pyroelectricity in polyvinylidene fluoride—A model. J. Appl. Phys. 1978; 49: 4992.

[2] D.K. Das-Gupta. On the nature of pyroelectricity in polyvinylidene fluoride. Ferroelectrics 1981; 33: 75.

[3] G. R. Harris, R. C. Preston, and A. S. DeReggi. The impact of piezoelectric PVDF on medical ultrasound exposure measurements, standards, and regulations. IEEE Trans. Ultrason., Ferroelect., Freq. Contr. 2000; 47(6): 1321.

[4] F. Stuart Foster, K. A. Harasiewicz, M. D. Sherar. A History of Medical and Biological Imaging with Polyvinylidene Fluoride (PVDF) Transducers. IEEE Trans. Ultrason., Ferroelect., Freq. Contr. 2000; 47(6): 1363.

[5] W. P. Mason. Technical Digests: An Electromechanical Representation of a Piezoelectric Crystal Used As A Transducer. Bell System Technical Journal 1935; 14(4): 718.

[6] A. L. Robinson. Flexible PVF2 film: An exceptional polymer for transducers. Science 1978; 200: 1371

[7] E. Passaglia, M. Broadhurst, E. DiMarzio, and I. Sanchez. High-polymer physics. Physics Today 1984; 37: 48.

[8] I. Amato. Fantastic plastic. Sci. News 1989; 136: 328.

[9] G. M. Sessler. Piezoelectricity in polyvinylidenefluoride. J. Acoust. Soc. Amer. 1981; 70: 1596.

[10] S. Lanceros-Mendez, M. V. Moreira, J. F. Mano, V. H. Schmidt and G. Bohannan. Dielectric Behavior in an Oriented β -PVDF Film and Chain Reorientation Upon Transverse Mechanical Deformation. Ferroelectrics 2002; 273(1): 15.

[11] Y. Roh, V. V. Varadan, V. K. Varadan. Characterization of All the Elastic, Dielectric, and Piezoelectric Constants of Uniaxially Oriented Poled PVDF Films . IEEE Trans. Ultrason., Ferroelect., Freq. Contr. 2002; 49(6): 836.

[12] V. Sencadas, S. Lanceros-Méndez, J.F. Mano . Characterization of poled and non-poled β -PVDF films using thermal analysis techniques . Thermochimica Acta 2004; 424: 201.

[13] R. Singh, J. Kumar, R. K. Singh, A. Kaur, R. Sinha, N. Gupta. Low frequency ac conduction and dielectric relaxation behavior of solution and uniaxially streched poly(vinylidene fluoride) films. Polymer 2006; 47: 5919.

[14] A. Vinogradov, V. Schmidt, G. Tuthill, G. Bohannan. Damping and electromechanical energy losses in the piezoelectric polymer PVDF . Mechanics of Materials 2004; 36: 1007.

[15] M. Grimau, E. Laredo, A. Bello, N. Suarez. Correlation between Dipolar TSDC and AC Dielectric

Spectroscopy at the PVDF Glass Transition. J. Polym. Sci. B: Polym Phys 1997; 35: 2483.

[16] V. Kochervinskii, I. Malyshkina, N. Gavrilova, S. Sulyanov, N. Bessanova. Peculiarities of piezoelectric relaxation in poly(vinylidene fluoride) with different thermal history. J. of Non-Crystaline Solids 2007; 352: 4443.

[17] R. Gregorio, E. Ueno. Effect of crystalline phase, orientation and temperature on the dielectric properties of poly (vinylidene fluoride). J. Material Science 1999; 34: 4489.

[18] E. Tuncer, M. Wegener and R. Gerhard-Multhaupt. Distribution of relaxation times in α-phase polyvinylidene fluoride. J. Non-Cryst. Solids 2005; 351; 2917.

[19] S. Sokhanvar, M. Packirisamy, J. Dargahi. A multifunctional PVDF-based tactile sensor for minimally invasive surgery. Smart Mater. Struct. 2007; 16: 989.

[20] Zuo-Guang Ye . Handbook of dielectric, piezoelectric and ferroelectric materials . Woodhead Publishing Limited and CRC Press LLC . 2008.

[21] W. P. Mason. Piezoelectric crystals and their application to ultrasonics. Van Nostrand Reinhold. 1964.

[22] R. R. Mocellini, G. I. Zelada-Lambri, O. A. Lambri, C.L. Matteo, P.A. Sorichetti. Electro-rheological Description of Liquid and Solid Dielectrics Applied to Two-phase Polymers, IEEE Transactions on Dielectrics and Electrical Insulation 2006; 13(6): 1358.

[23] P.A. Sorichetti, C.L. Matteo. Low-frequency dielectric measurements of complex fluids using high-frequency coaxial sample cells, Measurement 2007; 40: 437.

[24] J. Feinstein et al., UHF and Microwave Devices, Chapter 12, in: D.G. Fink (Ed.), Electronics Engineers Handbook, 4th edition, McGraw-Hill, New York, 1997.

[25] D. Damjanovic. Ferroelectric, dielectric and piezoelectric properties of ferroelectric thin films and ceramics. Rep. Prog. Phys. 1998; 61: 1267.

[26] K. Uchino. Loss Mechanisms in Piezoelectrics: How to Measure Different Loss Separately. IEEE Trans. Ultrason., Ferroelect., Freq. Contr. 2001; 48(1): 307.

[27] J.P. Runt, J.J. Fitzgerald. Dielectric Spectroscopy of Polymeric Materials: Fundamentals and Applications. American Chemical Society. 1997.

[28] S. Havriliak, S. Negami. A complex plane analysis of a-dispersions in some polymer systems. J.Polym.Sci., Polym. Symp. 1966; 14: 99.

Table Captions

Table 1. Havriliak-Negami parameters for the main relaxation peak at each measured temperature for a free sample.

Table 2. Havriliak-Negami parameters for the main relaxation peak at each measured temperature for a clamped sample.

Figure Captions

Figure 1. Real part of the relative complex permittivity for a free sample. Symbols: experimental data. Solid lines: HN function with the fitting parameters from table 1.

Figure 2. Imaginary part of the relative complex permittivity for a free sample. Symbols: experimental data. Solid lines: HN function with the fitting parameters from table 1.

Figure 3. Real part of the relative complex permittivity for a clamped sample. Symbols: experimental data. Solid lines: HN function with the fitting parameters from table 2.

Figure 4. Imaginary part of the relative complex permittivity for a clamped sample. Symbols: experimental data. Solid lines: HN function with the fitting parameters from table 2.

Figure 5. Cole-Cole plot (imaginary vs. real part of the complex permittivity) for a free sample. Symbols: experimental data. Solid lines: HN function with the fitting parameters from table 1.

Figure 6. Cole-Cole plot (imaginary vs. real part of the complex permittivity) for a clamped sample. Symbols: experimental data. Solid lines: HN function with the fitting parameters from table 2.

Figure 7. Real part of the difference between the free and clamped permittivities.

Figure 8. Imaginary part of the difference between the free and clamped permittivities.

Figure 9. Arrhenius plot of the characteristics times for a free sample. k_b is the Boltzmann constant.

Figure 10. Arrhenius plot of the characteristics times for a clamped sample. k_b is the Boltzmann constant.

TABLE 1					
T (K)	γ	δ	ε_{HF}	$\Delta\varepsilon$	τ_0 (μs)
284.1	0.78	0.40	2.55	2.85	2.10
288.3	0.86	0.19	2.79	5.10	0.79
294.1	0.90	0.22	2.54	5.41	0.49
299.1	0.86	0.25	2.44	5.28	0.31
304.1	0.18	0.28	2.34	6.24	0.37
308.7	0.78	0.27	2.45	7.70	0.12

TABLE 2

T (K)	γ	δ	ε_{HF}	Δε	τ_0 (μs)
279.3	0.56	0.47	1.98	5.88	2.00
284.1	0.57	0.49	2.09	5.81	1.10
288.3	0.57	0.54	2.16	5.84	0.57
294.1	0.62	0.46	1.95	5.94	0.43
299.1	0.60	0.50	1.88	6.15	0.24
304.1	0.63	0.46	1.81	6.15	0.18
308.7	0.61	0.54	1.89	6.15	0.09

Figure1

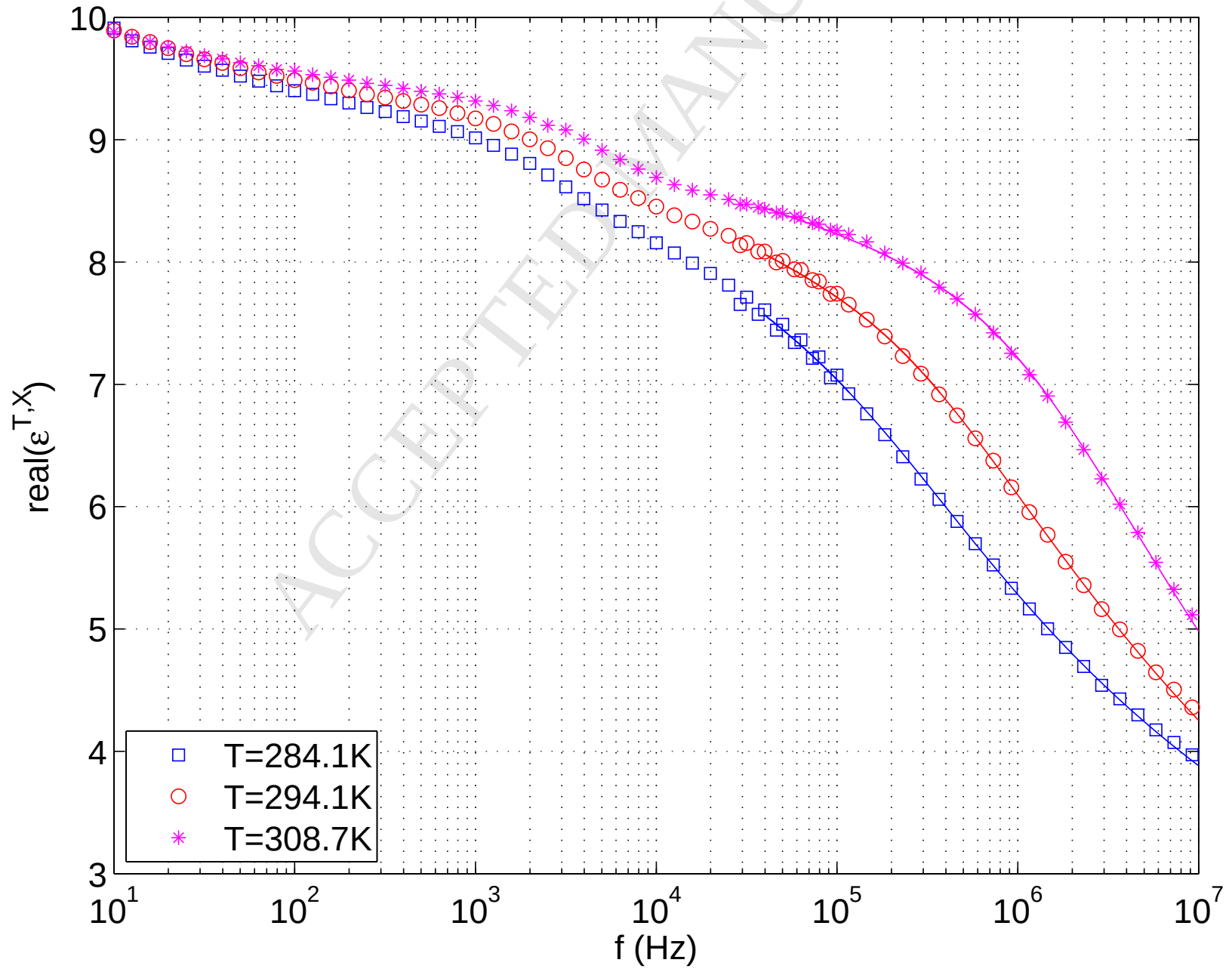

Figure2

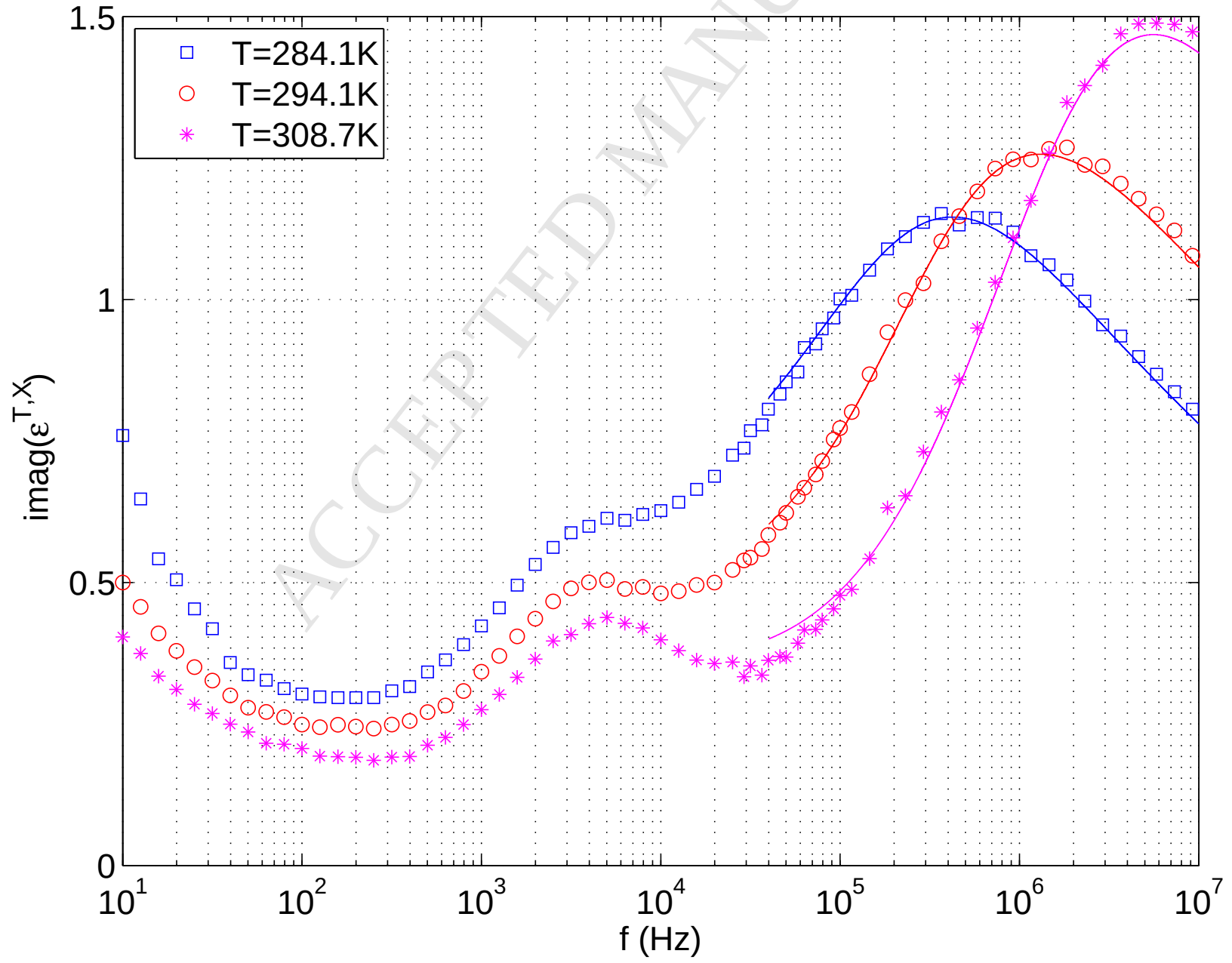

Figure3

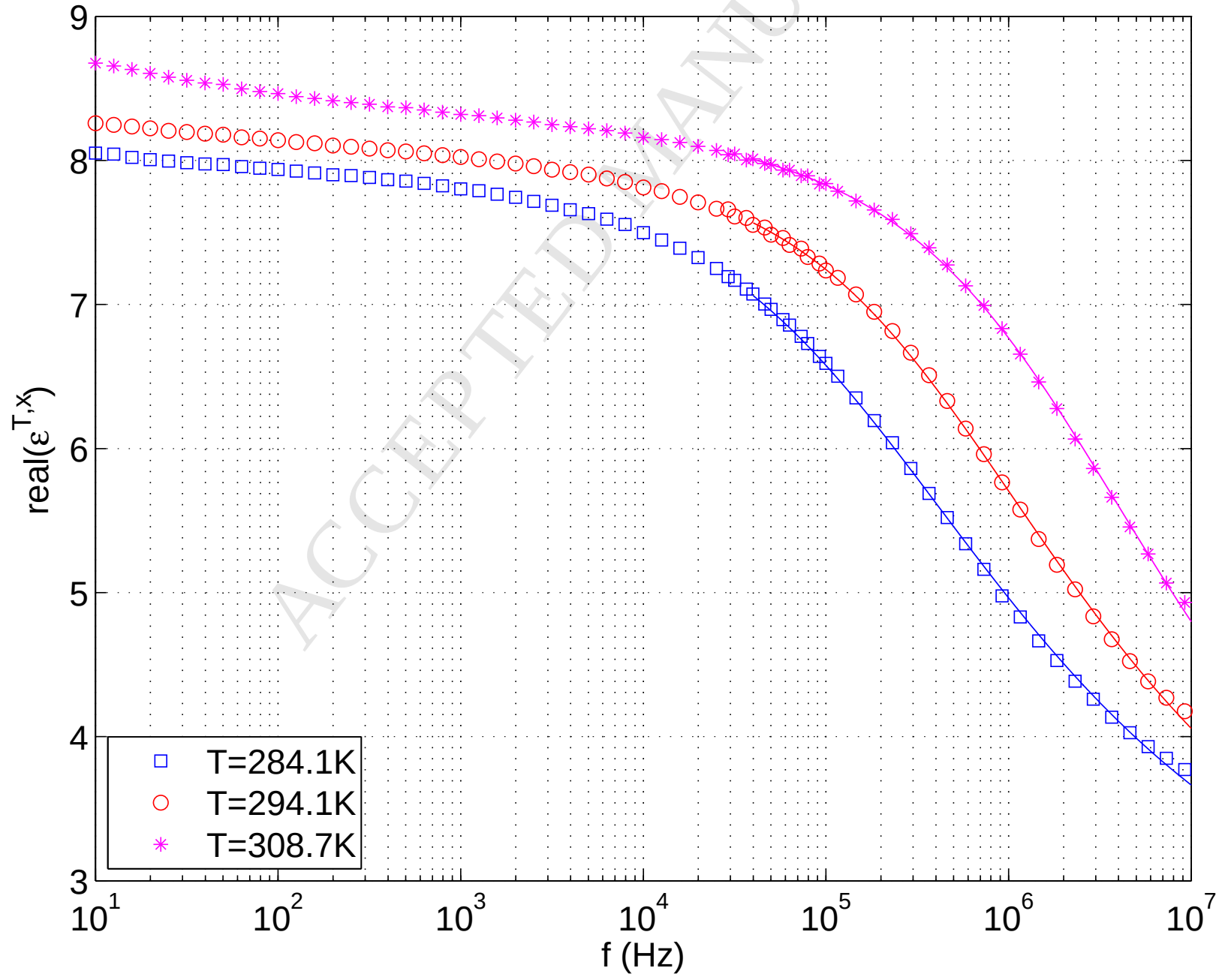

Figure4

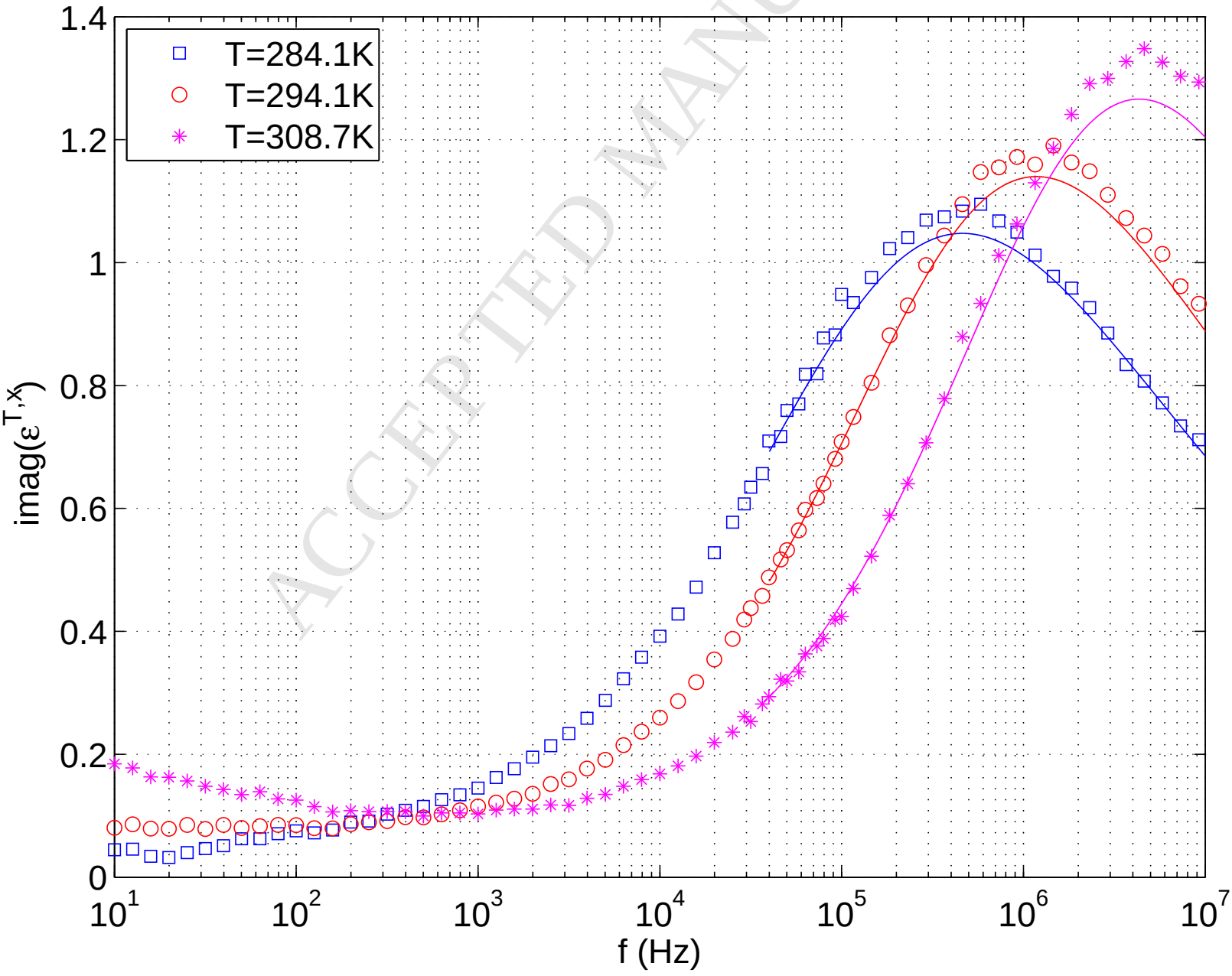

Figure5

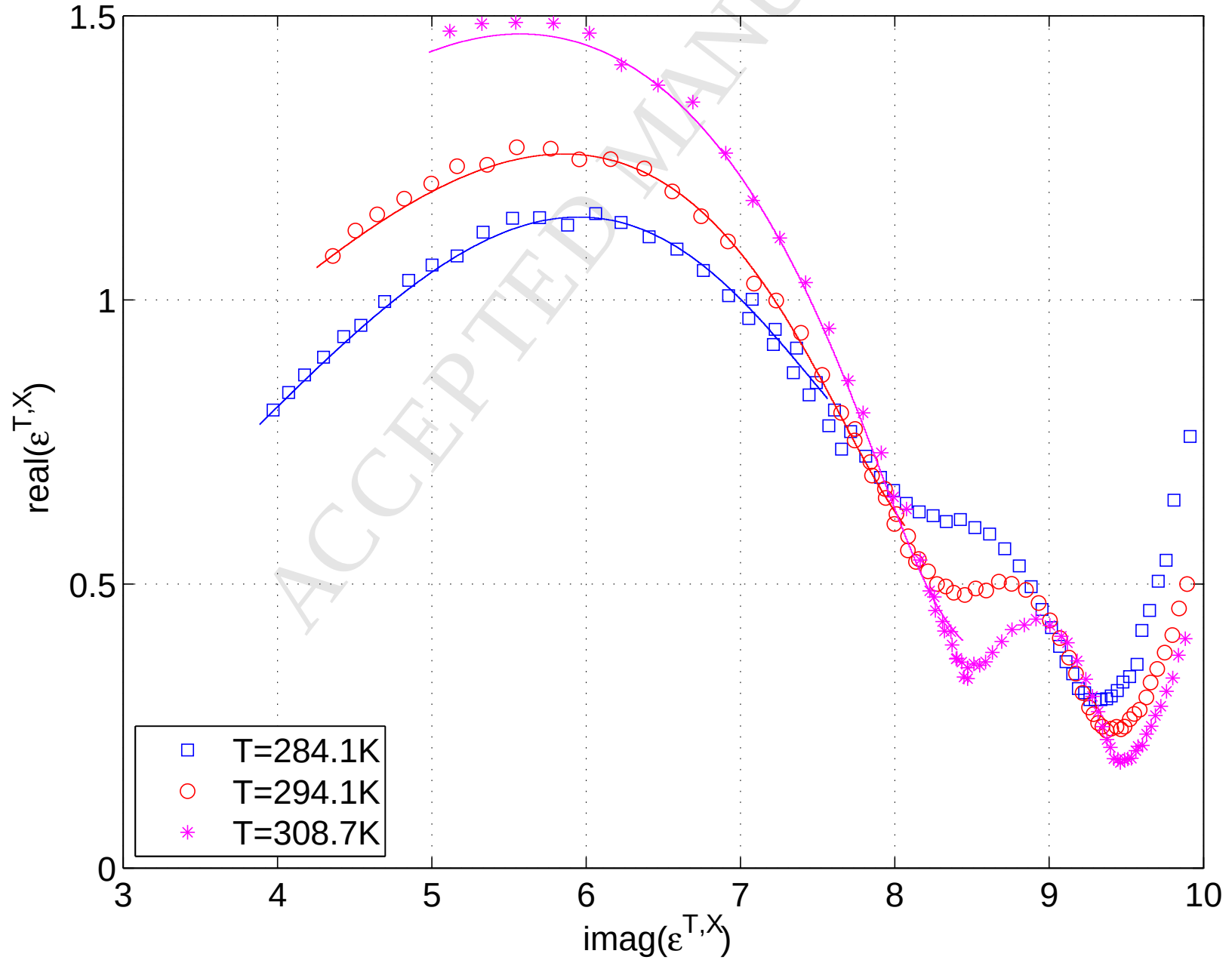

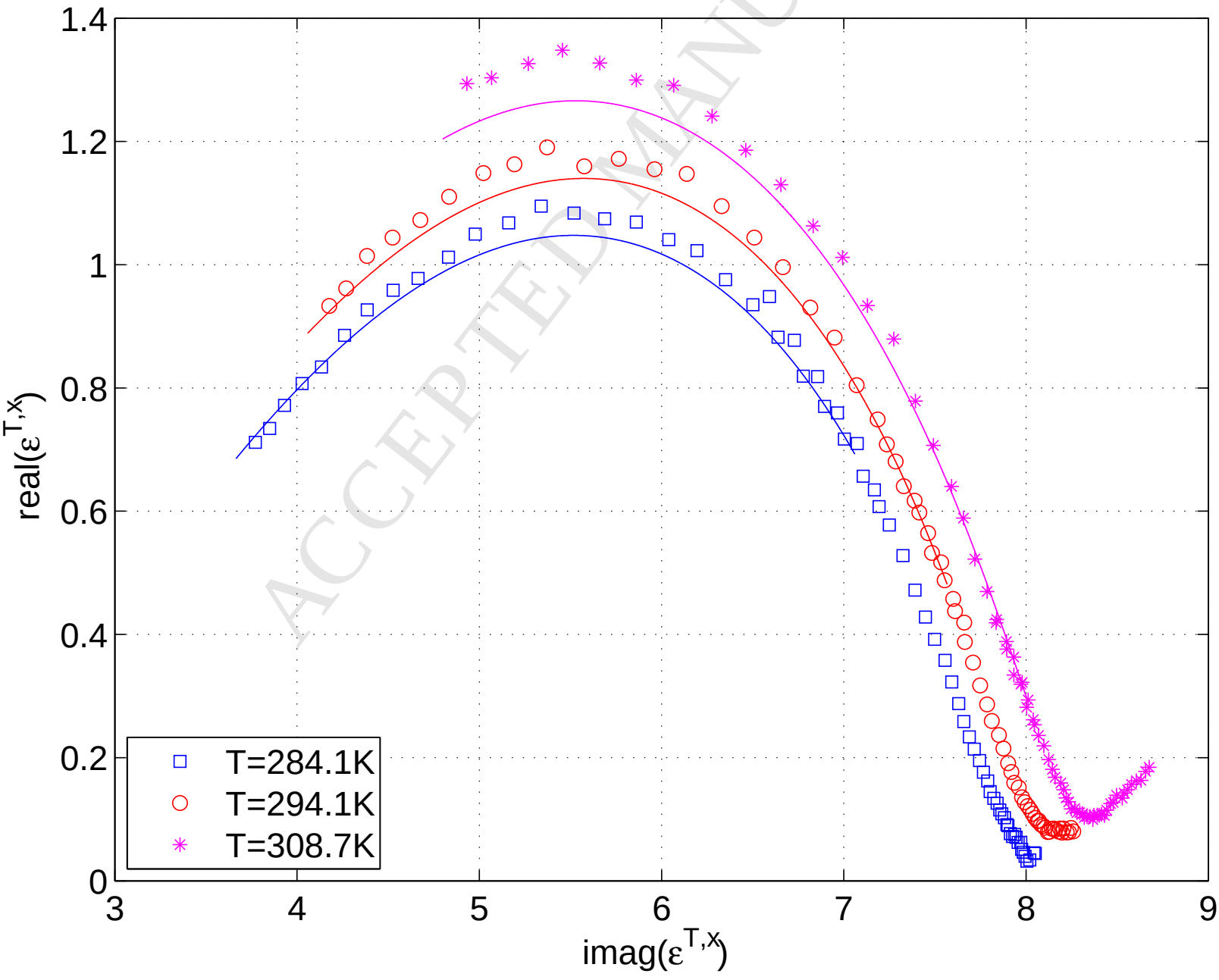

Figure7